Available online at www.sciencedirect.com
ScienceDirect
Dyes and Pigments 77 (2008) 335–342
DYES and PIGMENTS
www.elsevier.com/locate/dyepig

Star-shaped, nonlinear optical molecular glass bearing 2-(3-cyano-4-{4-[ethyl-(2-hydroxy-ethyl)-amino]-phenyl}-5-oxo-1-{4-[4-(3-oxo-3-phenyl-propenyl)-phenoxy]-butyl}-1,5-dihydro-pyrrol-2-ylidene)-malononitrile

Min Ju Cho, Sang Kyu Lee, Dong Hoon Choi*, Jung-Il Jin**

Department of Chemistry, Center for Electro- and Photo-responsive Molecules, Korea University, 5 Anamdong Sungbuk-gu, Seoul 136-701, South Korea

Received 18 February 2007; received in revised form 27 May 2007; accepted 6 June 2007
Available online 21 June 2007

Abstract

Novel, photocrosslinkable, star-shaped molecules have been synthesized by attaching a tricyanopyrroline (TCP)-based chromophore to 6-(4-{1,1-bis-[4-(5-carboxy-pentyloxy)-phenyl]-ethyl}-phenoxy)-hexanoic acid. The chromophore 2-(3-cyano-4-(4-diethylamino-phenyl)-5-oxo-1-{4-[4-(3-oxo-3-phenyl-propenyl)-phenoxy]-butyl}-1,5-dihydro-pyrrol-2-ylidene)-malononitrile is a second-order nonlinear optical active compound and bears a chalcone moiety that is sensitive to UV light ($\lambda = 320-350$ nm) for $2\pi + 2\pi$ photocycloaddition. The resultant molecules exhibited good processability and showed 29–37 pm/V of the maximum electro-optic coefficient at 1300 nm.

Keywords: Tricyano-pyrroline chromophore; Star-shaped molecule; Photocrosslinkable chromophore; Electro-optic effect; Thermal stability; Cycloaddition

1. Introduction

Over the past two decades, researchers have shown a great deal of interest in organic nonlinear optical (NLO) active chromophores and polymeric composites [1–3]. Polymeric materials have a strong potential for use in telecommunications, digital signal processing, phased array radar, THz generation, and many other applications as active materials in photonic microdevices [4–7]. This interest has given rise to the need for materials with better electro-optic (EO) properties, both at the molecular level and as processed materials. Organic NLO material systems are advantageous because of factors such as a high NLO susceptibility, a fast response time, a low dielectric constant, small dispersion in the refractive index, structural flexibility, and ease of material processing [8–10]. Recently, Jen's group reported a significantly high EO coefficient of around 200–262 pm/V at 1300 nm, using a dialkylaminotetraene-type chromophore in amorphous polycarbonate; this is the highest value reported thus far [11].

However, there still remains a strong need to improve the thermal stability of these materials in order to fulfill the requirements for multilayer fabrication processes and long-term device operations. Hence, the thermal crosslinking reaction is often adopted for stabilizing the bulk acentric ordering of the NLO molecular lattice [12–15]. However, thus far, there have only been a few reports on photocrosslinkable NLO materials.

Very recently, the strong potential of tricyano-pyrroline (TCP) chromophores and their detailed microscopic analysis data were demonstrated [16]. In particular, the electron-accepting properties of TCP moiety are considerably stronger than those of tricyanofuran (TCF). Although there were many reports about photosensitive NLO material systems, photocrosslinking was rather rarely employed for lattice-hardening processes [17,18].

This report suggests that photocrosslinking provides a facile method to tune the thermal stability of the EO effect.

* Corresponding author. Tel.: +82 2 3290 3140; fax: +82 2 924 3141.
** Corresponding author. Tel.: +82 2 3290 3123; fax: +82 2 3290 3121.
E-mail addresses: dhchoi8803@korea.ac.kr (D.H. Choi), jijin@korea.ac.kr (J.-I. Jin).

0143-7208/$ - see front matter © 2007 Elsevier Ltd. All rights reserved.
doi:10.1016/j.dyepig.2007.06.001

We report the synthesis and characterization of new photocrosslinkable NLO star-shaped molecules bearing TCP-based chromophores. One molecule contains a photochemically inert TCP chromophore and the other comprises a photocrosslinkable TCP chromophore. This is a new synthetic study for preparing an NLO chromophore with a photocrosslinkable unit in one molecule and an NLO star-shaped molecule exhibiting tunable thermal stability. A real-time pole-and-probe technique permits us to synchronously monitor the EO signal even during light irradiation. The rising behavior and dynamic stability of the EO signal of dendrimer samples are investigated under UV light illumination.

2. Experimental

2.1. Materials and measurements

All commercially available starting materials were purchased from Aldrich or Acros Co. and used without further purification unless otherwise stated. All solvents used in this study were freshly dried under the standard distillation method.

A chalcone moiety, **1** and core unit, **2** were synthesized by using a modified approach to a published method [19,20].

^{1}H NMR spectra were recorded on a Varian Mercury NMR 300 MHz spectrometer using deuterated chloroform or DMSO (Cambridge Isotope Laboratories, Inc.). Elemental analyses were performed using an EA1112 (Thermo Electron Corp.) elemental analyzer. Thermal properties were studied under a nitrogen atmosphere on a Mettler DSC 821^e instrument. Thermogravimetric analysis was performed using Mettler TGA50 (temperature rate 10 °C under N_2). Absorption analysis was performed with UV–vis spectrometer (HP 8453, PDA type, $\lambda = 190-1100$ nm). He–Cd laser (Melles Griot, $\lambda = 325$ nm, Model 3074-M-A01) and Xenon lamp equipped with monochromator (Thermo Oriel, Model 6C921, 1 kW) were utilized as an excitation source.

Spectroscopic ellipsometry measurement to determine the refractive indices at various wavelengths was performed on the thin film using a Woollam VASE model with an autoretarder. EO signal was monitored by real-time pole-and-probe method that is a modified simple reflection method [20–22]. The linear EO coefficient, "r_{33}" of the poled film was calculated using the ratio of the amplitude of EO modulation (I_m) and the intensity of incident light where phase retardation is 90° between TE and TM mode (I_c). In order to induce photocrosslink, we focused pump beam from He–Cd laser on the reflected spot of the incident diode laser (LaserMax, $\lambda = 1300$ nm, 10 mW) during poling.

2.2. Synthesis

2.2.1. Synthesis of compound *3*

4-Cyano-5-dicyanomethylene-3-hydroxy-2-oxo-3-pyrroline disodium salt (6.90 g, 30.00 mmol), 2-(*N*-ethylanilino)ethyl acetate (7.25 g, 35.00 mmol), and acetic anhydride (2.42 g, 30 wt% aniline) were dissolved in 50 mL of DMF under argon. The reaction mixture was cooled in an ice bath. $POCl_3$ (4.59 g, 30.00 mmol) was added dropwise over 0.5 h. The color of the reaction mixture turned blue and the mixture was stirred for 6 h at room temperature. Precipitation was done by pouring the reaction mixture into ice water. The solid was filtered and dried to yield 8.76 g (77%) of dark blue solid.

^{1}H NMR (300 MHz, DMSO-d_6): δ (ppm) 12.56 (s, 1H), 8.30 (d, $J = 8.7$ Hz, 2H), 7.02 (d, $J = 8.7$ Hz, 2H), 4.22 (t, 2H), 3.77 (t, 2H), 3.58 (q, 2H), 1.96 (s, 3H), 1.15 (t, 3H).

^{13}C NMR (DMSO-d_6): δ (ppm) 171.010, 168.892, 159.192, 153.621, 144.961, 133.512, 116.119, 114.540, 113.763, 113.457, 112.632, 95.039, 61.840, 58.348, 49.105, 46.142, 21.356, 12.846.

EA analysis: Calcd for $C_{20}H_{17}N_5O_3$: C, 63.99; H, 4.56; N, 18.66; O, 12.79; found: C, 63.67; H, 4.51; N, 18.08.

HRMS: *m/z* Calcd for $C_{20}H_{17}N_5O_3$ $[M + Na]^+$, 398.1229; found, 398.1218.

2.2.2. Synthesis of compound *4a*

Compound **3** (3.75 g, 10.00 mmol) and sodium carbonate (0.529 g, 5.00 mmol) were mixed in 50 mL of DMF under argon. After heating the solution at 90 °C, 1-bromobutane (2.05 g, 15.00 mmol) was added dropwise and the reaction mixture was stirred for 24 h. It was poured into ice water to obtain the greenish solid product. The solid was filtered and dried at 60 °C *in vacuo*. The resulting product was purified by silica gel column chromatography (EtOAc:chloroform = 1:9, v/v) to yield 3.47 g (80%) of green solid.

^{1}H NMR (300 MHz, $CDCl_3$): δ (ppm) 8.50 (d, $J = 8.7$ Hz, 2H), 6.84 (d, $J = 8.7$ Hz, 2H), 4.30 (t, 2H), 4.08 (t, 2H), 3.74 (t, 4H), 3.59 (q, 2H), 2.06 (s, 3H), 1.63–1.72 (m, 2H), 1.35–1.46 (m, 2H), 1.29 (t, 3H), 0.98 (t, 3H).

^{13}C NMR ($CDCl_3$): δ (ppm) 170.87, 167.17, 155.56, 153.190, 142.607, 133.830, 116.295, 113.668, 113.158, 112.934, 111.613, 96.434, 61.132, 60.661, 49.033, 46.245, 41.709, 31.552, 20.959, 19.638, 13.765, 12.498.

EA analysis: Calcd for $C_{24}H_{25}N_5O_3$: C, 66.81; H, 5.84; N, 16.23; O, 11.12; found: C, 66.82; H, 5.80; N, 16.10.

HRMS: *m/z* Calcd for $C_{24}H_{25}N_5O_3$ $[M + Na]^+$, 454.1855; found, 454.1853.

2.2.3. Synthesis of compound *4b*

Compound **3** (3.75 g, 10.00 mmol) and sodium carbonate (0.529 g, 5.00 mmol) were mixed in 50 mL of DMF under argon. After heating the solution at 90 °C, compound **1** (3.59 g, 10.00 mmol) in 20 mL of DMF was added dropwise and the reaction mixture was stirred for 24 h. It was poured into ice water to obtain the blue solid product. The resulting product was purified by silica gel column chromatography (EtOAc:chloroform = 1:7, v/v) to yield 4.22 g (65%) of green solid.

^{1}H NMR (300 MHz, $CDCl_3$): δ (ppm) 8.49 (d, $J = 8.7$ Hz, 2H), 8.01 (d, $J = 8.7$ Hz, 2H), 7.76 (d, $J = 15.6$ Hz, 1H), 7.59 (d, $J = 8.7$ Hz, 2H), 7.47–7.60 (m, 3H), 7.41 (d, $J = 15.6$ Hz, 1H), 6.92 (d, $J = 8.7$ Hz, 2H), 6.83 (d, $J = 8.7$ Hz, 2H), 4.29 (t, 2H), 4.17 (t, 2H), 4.07 (t, 2H), 3.73 (t, 4H), 3.58 (q, 2H), 2.05 (s, 3H), 1.88–1.97 (m, 4H), 1.28 (t, 3H).

^{13}C NMR ($CDCl_3$): δ 190.751, 170.900, 167.276, 160.996, 155.566, 153.249, 144.856, 142.616, 138.672, 133.941, 132.751, 130.459, 128.759, 128.608, 127.870, 119.977, 116.358, 115.105, 113.629, 113.235, 112.963, 111.487, 96.532, 67.277, 61.118, 60.899, 49.062, 46.279, 41.534, 26.506, 26.005, 20.988, 12.532.

EA analysis: Calcd for $C_{39}H_{35}N_5O_5$: C, 71.65; H, 5.40; N, 10.71; O, 12.24; found: C, 72.44; H, 5.43; N, 11.36.

HRMS: *m/z* Calcd for $C_{39}H_{35}N_5O_5$ $[M + Na]^+$, 676.2536; found, 676.2543.

2.2.4. Synthesis of compound *5a*

Compound **4a** (3.15 g, 7.30 mmol) was dissolved in 20 mL of THF. Aqueous solution of HCl (10 mL, 3 N) was added and the mixture was stirred at 80 °C for 12 h. After cooling to room temperature, 100 mL of water was added to precipitate out the product. The product collected by filtration, washed, and dried. The crude product was purified by silica gel column chromatography (EtOAc:chloroform = 1:3, v/v) to yield 2.46 g (86%) of green solid.

^{1}H NMR (300 MHz, $CDCl_3$): δ (ppm) 8.46 (d, $J = 8.7$ Hz, 2H), 6.87 (d, $J = 8.7$ Hz, 2H), 3.99 (t, 2H), 3.92 (q, 2H), 3.69 (t, 4H), 3.66 (q, 2H), 2.27 (t, 1H, OH), 1.59–1.70 (m, 2H), 1.33–1.45 (m, 2H), 1.30 (t, 3H), 0.97 (t, 3H).

^{13}C NMR ($CDCl_3$): δ 167.130, 155.833, 153.938, 141.247, 133.713, 116.116, 113.925, 113.502, 113.410, 111.997, 93.797, 60.214, 59.068, 52.793, 46.877, 41.646, 31.470, 19.618, 13.746, 12.386.

EA analysis: Calcd for $C_{22}H_{23}N_5O_2$: C, 67.85; H, 5.95; N, 17.98; O, 8.22; found: C, 67.81; H, 5.96; N, 17.92.

HRMS: *m/z* Calcd for $C_{22}H_{23}N_5O_2$ $[M + Na]^+$, 412.1749; found, 412.1749.

2.2.5. Synthesis of compound *5b*

Compound **4a** (3.53 g, 5.40 mmol) was dissolved in 20 mL of THF. Aqueous solution of HCl (10 mL, 3 N) was added and the mixture was stirred at 80 °C for 12 h. After cooling to room temperature, 100 mL of water was added slowly to precipitate out the product. The product collected by filtration was washed and dried. The crude product was purified by silica gel column chromatography (EtOAc:chloroform = 1:2, v/v) to yield 2.68 g (81%) of blue solid.

^{1}H NMR (300 MHz, $CDCl_3$): δ (ppm) 8.42 (d, $J = 8.7$ Hz, 2H), 8.01 (d, $J = 8.7$ Hz, 2H), 7.67 (d, $J = 15.6$ Hz, 1H), 7.54 (d, $J = 8.7$ Hz, 2H), 7.48–7.59 (m, 3H), 7.37 (d, $J = 15.6$ Hz, 1H), 6.89 (d, $J = 8.7$ Hz, 2H), 6.80 (d, $J = 8.7$ Hz, 2H), 4.15 (t, 2H), 4.08 (t, 2H), 3.93 (q, 2H), 3.67 (t, 4H), 3.60 (q, 2H), 2.26 (t, 1H, OH), 1.85–1.94 (m, 4H), 1.26 (t, 3H).

EA analysis: Calcd for $C_{37}H_{33}N_5O_4$: C, 72.65; H, 5.44; N, 11.45; O, 10.46; found: C, 71.30; H, 5.31; N, 10.58.

HRMS: *m/z* Calcd for $C_{37}H_{33}N_5O_4$ $[M + Na]^+$, 634.2430; found, 634.2421.

2.2.6. Synthesis of compound *6a*

Compound **2** (0.65 g, 1.00 mmol) and compound **5a** (1.83 g, 3.00 mmol) were dissolved in 50 mL CH_2Cl_2. DPTS (0.88 g, 3.00 mmol) and 0.62 g of *N*,*N*′-dicyclohexylcarbodiimide (DCC, 3.00 mmol) were added to the mother solution. The reaction mixture was allowed to stir at room temperature for 24 h under argon. Repeated dissolution and filtration removed most of the resultant urea. The filtered CH_2Cl_2 solution was then added dropwise to the stirring methanol. The precipitate was collected and the resulting product purified by silica gel column chromatography (EA:chloroform, 1:6, v/v) to yield 1.52 g (86%) of blue solid. $T_g = 71$ °C.

^{1}H NMR (300 MHz, $CDCl_3$): δ (ppm) 8.48 (d, $J = 8.7$ Hz, 6H), 6.97 (d, $J = 8.7$ Hz, 6H), 6.84 (d, $J = 8.7$ Hz, 6H), 6.74 (d, $J = 8.7$ Hz, 6H), 4.30 (t, 6H), 4.04 (t, 6H), 3.89 (t, 6H), 3.73 (t, 6H), 3.57 (q, 6H), 2.32 (t, 6H), 2.08 (s, 3H), 1.68–1.78 (m, 6H), 1.60–1.70 (m, 12H), 1.32–1.49 (m, 12H), 1.27 (t, 9H), 0.96 (t, 9H).

^{13}C NMR ($CDCl_3$): δ (ppm) 173.498, 167.179, 157.096, 155.561, 153.224, 142.631, 141.907, 133.830, 129.745, 116.305, 113.687, 113.162, 112.973, 111.623, 96.488,

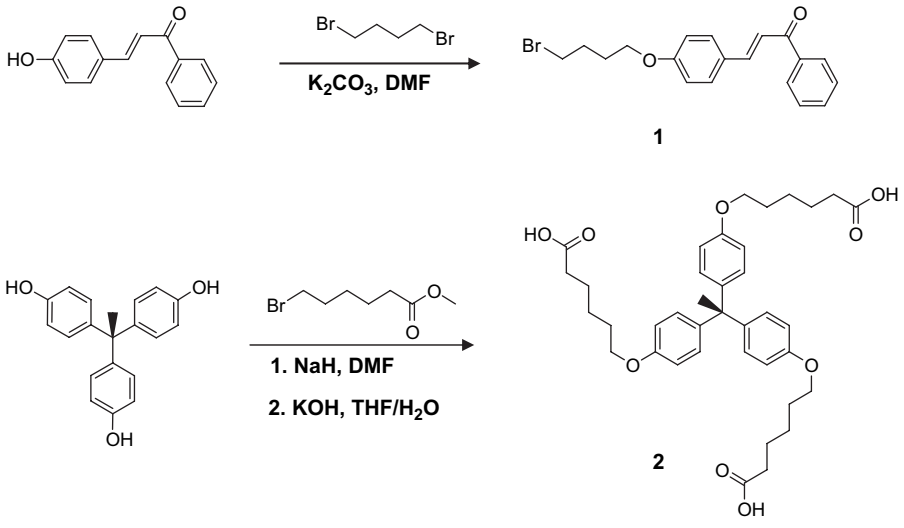

Scheme 1. Synthetic procedure of chalcone moiety, **1** and dendritic core, **2**.

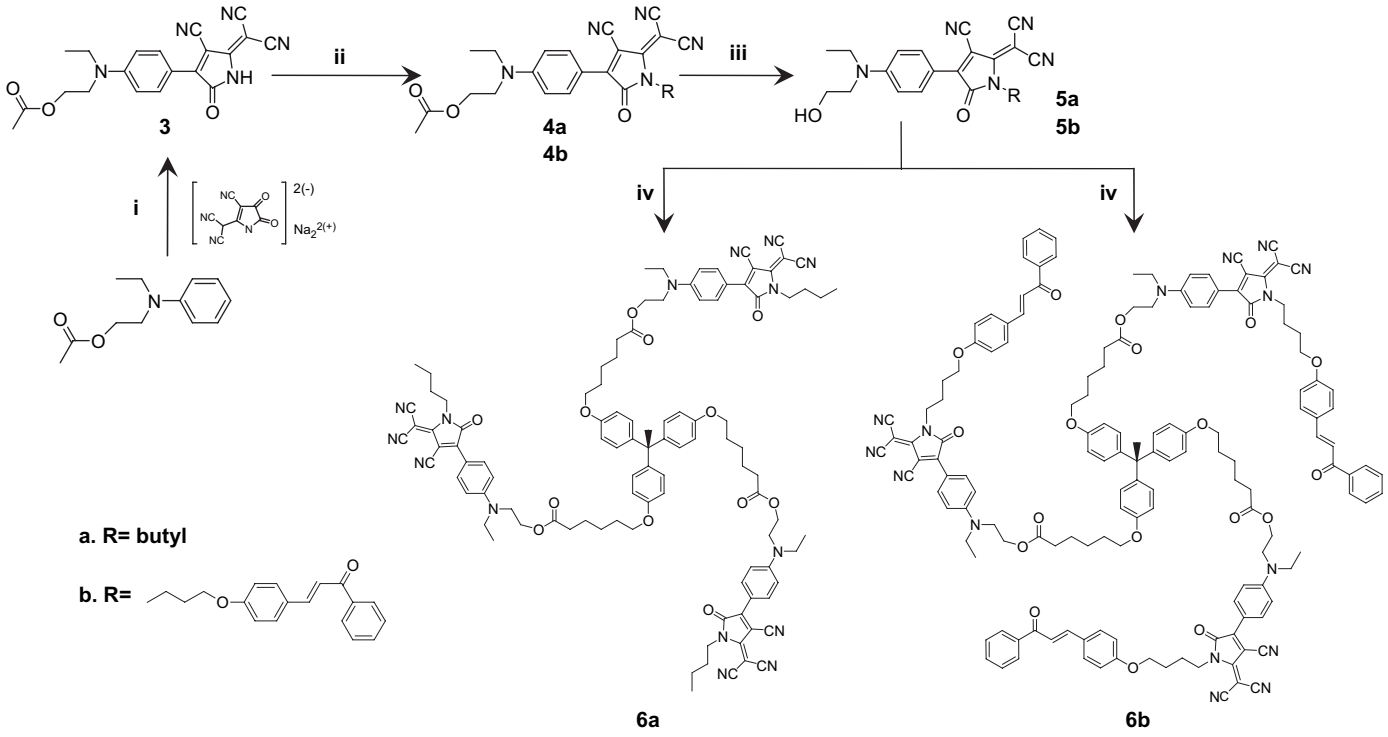

Scheme 2. Synthetic procedure for TCP-based NLO chromophores and their star-shaped molecules. Reagents and conditions: (i) $POCl_3$, DMF, acetic anhydride, 0 °C, 6 h; (ii) **a**: 1-bromobutane, Na_2CO_3, DMF, 90 °C, 24 h, **b**: compound **1**, Na_2CO_3, DMF, 90 °C, 24 h; (iii) HCl, THF, 80 °C, 12 h; (iv) compound **2**, DCC, DPTS, MC, rt, 24 h.

67.597, 61.026, 60.686, 50.714, 48.980, 46.124, 41.714, 34.136, 31.572, 30.931, 29.119, 25.801, 24.689, 19.647, 13.785, 12.507.

EA analysis: Calcd for $C_{104}H_{111}N_{15}O_{12}$: C, 70.85; H, 6.35; N, 11.92; O, 10.89; found: C, 70.75; H, 6.31; N, 11.81.

MALDI-TOF-MS *m/z* Calcd for $C_{104}H_{111}N_{15}O_{12}$ $[M+Na]^+$, 1784.8434; found, 1784.9726.

2.2.7. Synthesis of compound *6b*

Compound **2** (0.324 g, 0.50 mmol) and compound **5b** (0.917 g, 1.50 mmol) were dissolved in 50 mL CH_2Cl_2. DPTS (0.441 g, 1.50 mmol) and DCC (0.309 g, 1.50 mmol) were added to the mother solution. The reaction mixture was allowed to stir at room temperature for 24 h under argon. Repeated dissolution and filtration removed most of the resultant urea. The filtered CH_2Cl_2 solution was then added dropwise into methanol. The precipitate was collected and the resulting product purified by silica gel column chromatography (EA:chloroform, 1:5, v/v) to yield 0.94 g (77%) of blue solid. $T_g = 86$ °C.

^{1}H NMR (300 MHz, $CDCl_3$): δ (ppm) 8.47 (d, $J = 8.7$ Hz, 6H), 8.00 (d, $J = 8.7$ Hz, 6H), 7.75 (d, $J = 15.6$ Hz, 3H), 7.57 (d, $J = 8.7$ Hz, 6H), 7.46–7.60 (m, 9H), 7.40 (d, $J = 15.6$ Hz, 3H), 6.96 (d, $J = 8.7$ Hz, 6H), 6.90 (d, $J = 8.7$ Hz, 6H), 6.82 (d, $J = 8.7$ Hz, 6H), 6.73 (d, $J = 8.7$ Hz, 6H), 4.29 (t, 6H), 4.12 (t, 6H), 4.04 (t, 6H), 3.87 (t, 6H), 3.56 (q, 6H), 2.31 (t, 6H), 2.08 (s, 3H), 1.85–1.92 (m, 12H), 1.68–1.77 (m, 6H), 1.58–1.68 (m, 6H), 1.38–1.48 (m, 6H), 1.26 (t, 9H).

^{13}C NMR ($CDCl_3$): δ 190.620, 173.479, 167.203, 160.981, 157.091, 155.541, 153.307, 144.792, 142.437, 141.897, 138.604, 133.873, 132.742, 130.435, 129.740, 128.735, 128.565, 127.797, 119.880, 116.305, 115.076, 113.692, 113.648, 113.269, 113.022, 111.530, 96.221, 67.602, 67.272, 60.992, 60.627, 50.709, 48.975, 46.138, 41.476, 34.122, 30.921,29.109, 26.457, 25.976, 25.787, 24.675, 12.512.

Table 1
The physical properties and measured parameters of the star-shaped molecules, **6a** and **6b**

	λ_{max} (nm)	T_g (°C)	Dye conc. (wt%)	Transition temperature (°C)				EO property	
				Rising (T_{tr}^R)		Decaying (T_{tr}^D)		r_{33} (pm/V)[a] ($E_p = 70$ V/μm)	
				Pristine	UV-exposed	Pristine	UV-exposed	Pristine	UV-exposed
6a	629	71	63	74	–	64	–	32 37[b]	–
6b	634	86	46	79	92	80	94	29	23

[a] The refractive indices of **6a** and **6b** are 1.67 and 1.70, respectively.
[b] The sample was poled under 80 V/μm.

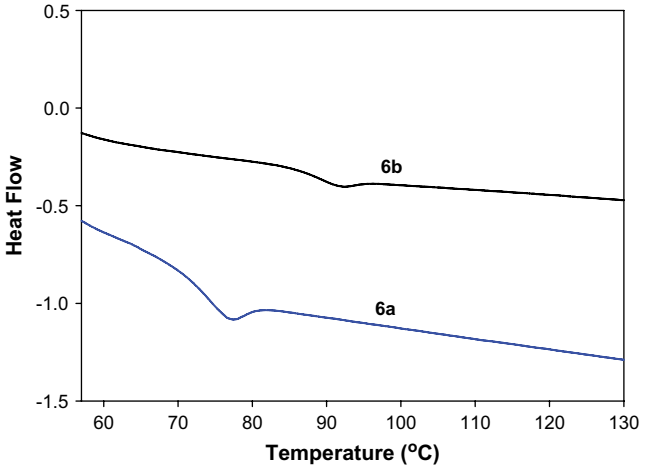

Fig. 1. DSC thermograms of **6a** and **6b**.

EA analysis: Calcd for $C_{149}H_{141}N_{15}O_{18}$: C, 73.65; H, 5.85; N, 8.65; O, 11.85; found: C, 73.10; H, 5.87; N, 8.54.

MALDI-TOF-MS *m/z* Calcd for $C_{149}H_{141}N_{15}O_{18}$ $[M+Na]^+$, 2451.0477; found, 2551.0900.

3. Results and discussion

3.1. Synthesis and materials

4-Hydroxychalcone was reacted with dibromobutane to obtain **1**, and a core unit with carboxylic acid groups in three arms was also synthesized (Scheme 1). The syntheses of 2-(1-butyl-3-cyano-4-{4-[ethyl-(2-hydroxy-ethyl)-amino]-phenyl}-5-oxo-1,5-dihydro-pyrrol-2-ylidene)-malononitrile (**5a**) and 2-(3-cyano-4-{4-[ethyl-(2-hydroxy-ethyl)-amino]-phenyl}-5-oxo-1-{4-[4-(3-oxo-3-phenyl-propenyl)-phenoxy]-butyl}-1,5-dihydro-pyrrol-2-ylidene)-malononitrile (**5b**) are illustrated in Scheme 2, including the structures of the resultant two star-shaped molecules. The butyl group in the secondary amine group of the pyrroline ring improves the solubility of the chromophore in organic solvents. While **5a** was photochemically inert, **5b** was photochemically active. In particular, **5b** was prepared to attach one photocrosslinkable group to the NLO chromophore, although the reaction yield was fairly low (~20%). It was sensitive to UV light ($\lambda = 300-360$ nm) and underwent $2\pi + 2\pi$ cycloaddition [23–25]. DCC catalyzed esterification was conducted to prepare **6a** and **6b** with a moderately high yield. The two star-shaped molecules were highly soluble in common organic solvents such as chloroform, THF, cyclopentanone, and DMF.

The net compositions (wt%) of the NLO chromophore and chalcone group are illustrated in Table 1. The glass transition temperatures of **6a** and **6b** are measured and also tabulated in Table 1. Compound **6b** has a higher T_g (=86 °C) than **6a**, which is due to the higher molar mass as well as the existence of a rigid chalcone group (see Fig. 1). In addition, the two dendrimers have a good film-forming property for fabricating thin films.

3.2. Absorption spectroscopy of *6a* and *6b*

The absorption spectra of **6a** and **6b** in the solution state are also illustrated in Fig. 2A. The absorption spectrum of **6a** illustrates an important feature in that a very sharp low-energy absorption edge ($\lambda = 700$ nm) is observed. The intrinsic optical loss in an NLO material that is attributable to chromophore absorption would be rather small at the communication wavelengths of 1.30 and 1.55 μm.

Moreover, it should be noted that absorption by the selected TCP-based NLO chromophore is weak at the wavelength ($\lambda = 330-343$ nm) at which absorption by the photocrosslinkable group is the maximum. Therefore, **6b** is thought to be sensitive to UV light for inducing the photocycloaddition reaction.

UV–vis absorption spectroscopy for the solution state revealed that **6a** and **6b** have absorption maxima at 629 nm and 634 nm, respectively; these absorption maxima commonly arise from the π–π* transition bands in the NLO unit. In particular, **6b** has another characteristic absorption maximum (λ_{max}) at 343 nm, which corresponds to the π–π* transition bands in the chalcone unit (see Fig. 2A). In Fig. 2B, we

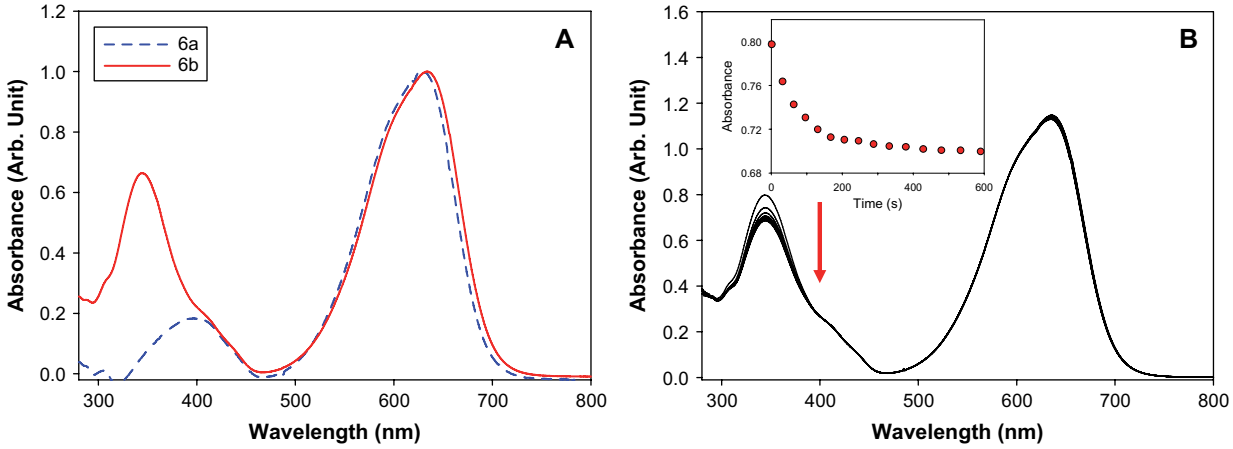

Fig. 2. UV–vis absorption spectra of **6a** and **6b**. (A) Spectra in solution state: **6a** (dotted line), **6b** (solid line). (B) Spectral change of **6b** during UV light irradiation.

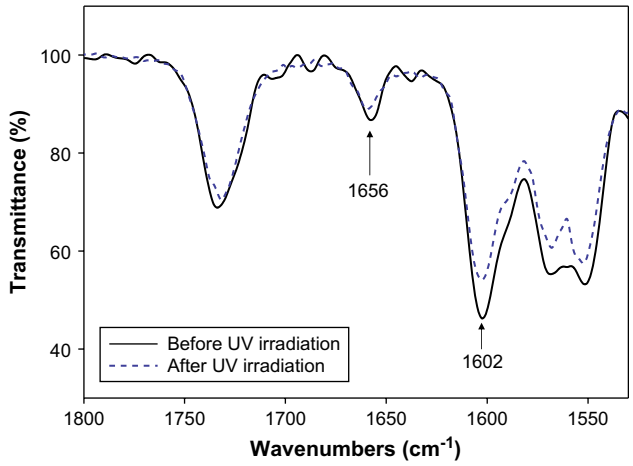

Fig. 3. Infrared spectral change of the **6b** films before and after UV light illumination. $\lambda_{ex} = 325$ nm.

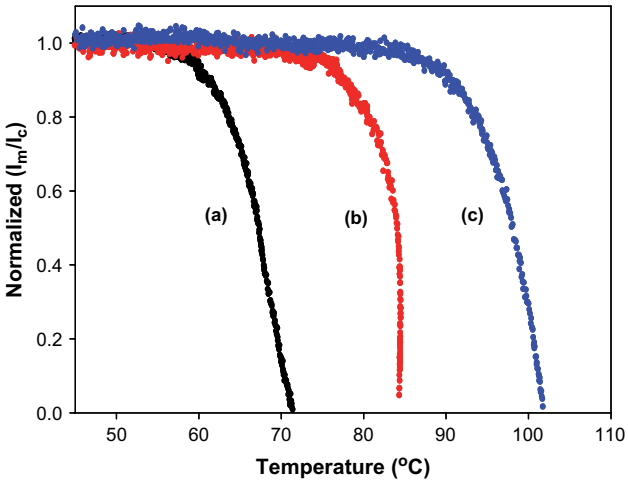

Fig. 5. Dynamic decaying behaviors of EO signal with the temperature. (a) Poled **6a** sample, (b) poled **6b** sample, (c) poled **6b** sample under UV exposure.

illustrated the absorption spectral change of **6b** during UV (Xe lamp with monochromator, $\lambda_{ex} = 340$ nm, $I = 10$ mW/cm^2) irradiation. The UV absorption changes at λ_{max} in **6b** caused by photoreaction were investigated using chloroform solution. The chalcone units underwent a crosslinking reaction by [2 + 2] cycloaddition between a UV-excited chalcone group and an unexcited chalcone group (ground state) on another. As the irradiation time increased, the absorbance at 343 nm decreased gradually and that at 634 nm was rather constant. In the inset figure, the dynamic decaying behavior of the absorbance at 343 nm is shown. The TCP-based chromophore used in this study showed significant persistence against the radical generated in the polymer.

3.3. Infrared spectroscopic study on photocrosslinking reaction

In order to monitor the photoreaction of the olefinic −C═C− double bonds of the chalcone group, we utilized FT-IR spectroscopy. Fig. 3 shows the localized FT-IR spectra of the **6b** sample. The spectra, plotted on an absolute transmittance scale in the range from 1800 to 1500 cm^{-1}, were recorded with the same sample before and after UV exposure. Indeed, significant changes occurred in the infrared spectra upon UV irradiation. The −C═C− stretching vibration mode at 1602 cm^{-1} is observed to decrease significantly due to UV exposure. The spectral band from the ethylenic double bond is normally superposed with the absorption bands of the double bonds in the benzene ring. In addition, the intensity of the C═O unsaturated ketone carbonyl stretching band at 1656 cm^{-1} decreases after UV exposure; further, a new band at 1664 cm^{-1}, attributed to a saturated ketone carbonyl stretching vibration, appears in the spectrum of the polymer after UV irradiation (see Fig. 3).

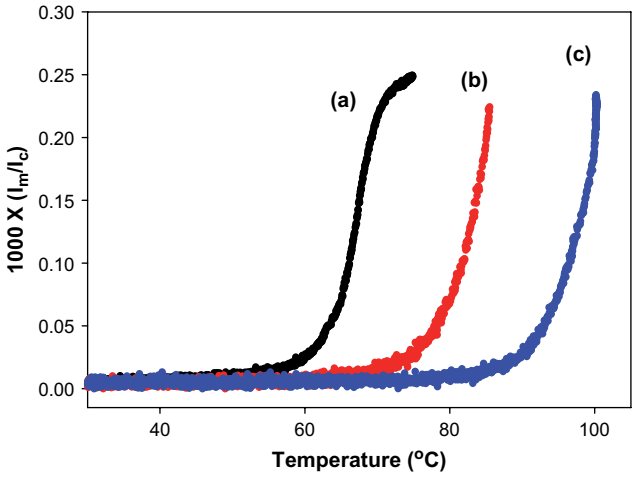

Fig. 4. Rising curves of EO signal during poling. (a) Pristine **6a** sample, (b) pristine **6b** sample, (c) UV-exposed **6b** sample.

3.4. Electro-optic properties of NLO molecular glasses

The EO coefficient (r_{33}) values were measured by a modified reflection technique [20–22]. We could monitor the variation of the EO signal (I_m/I_c) during heating, cooling, and UV illumination in the presence of a poling field. In order to investigate the effect of photocrosslinking, we prepared two sandwiched EO samples using **6a** and **6b**. In the case of **6b**, one of the sandwiched EO samples was the pristine sample, while the other was the sample that was exposed to 325 nm UV light (He–Cd laser $I = 25$ mW/cm^2) for 5 min before poling.

Curve (a) was obtained by poling the pristine **6a** sample (poling field: 70 V/μm) and curve (b) was obtained by poling the **6b** sample (see Fig. 4). From the UV-exposed **6b** sample, we could obtain curve (c). When poling the samples, a significant shift in the transition temperature (T_{tr}^R) of the rising curve was observed at a higher temperature in the UV-exposed **6b** sample (see Table 1). This is mainly attributed to the high degree of crosslinking between the chalcone moieties and the hardening of the matrix. Therefore, the **6b** sample underwent a photo-assisted lattice-hardening process after the illumination of monochromatic UV light ($\lambda_{ex} = 325$ nm).

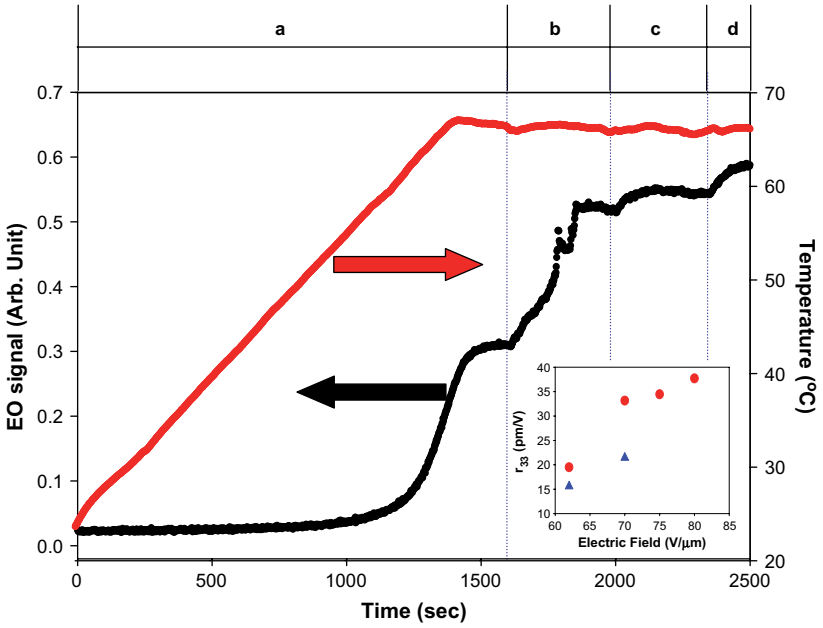

Fig. 6. Profile of EO signal during poling with the temperature and electric field. (a) 62 V/μm, (b) 70 V/μm, (c) 75 V/μm, (d) 80 V/μm. *Inset: electric field dependence of EO coefficient, r_{33}. (circle): **6a**, (triangle): **6b**.

The dynamic decaying behavior of the maximized EO signal was investigated in order to evaluate the thermal stability (see Fig. 5). One of the **6b** samples was poled at 70 V/μm during UV irradiation. The poled **6a** sample showed the lowest transition temperature at which the EO signal decreased abruptly. This indicates that the worst stability of the EO signal among the three different samples was shown by **6a**. Curve (c) was obtained from the sample that was exposed to UV irradiation at the maximum poling temperature for 5 min. Owing to the highly efficient lattice-hardening process induced by photocycloaddition, the **6b** sample showed clear evidence of the tunable thermal stability of the chromophore alignment. The UV-exposed **6b** sample showed a shift in the transition temperature (T_{tr}^{D}), which is similar to the trend of the transition temperature (T_{tr}^{R}) for the rising behavior shown in Fig. 4.

Further, under a relatively low poling field ($E_p = 70$ V/μm), all the pristine samples exhibited rather promising EO coefficients: 32 pm/V for **6a** and 29 pm/V for **6b**. Compound **6a** showed a higher EO coefficient as compared to **6b** because of lower T_g and a more facile orientation of the small chromophores in **6a**. As can be seen in Fig. 6, with careful variation in the temperature and poling field, we could obtain the maximum EO coefficient of **6a** around 37.0 pm/V under 80 V/μm.

In order to overcome the commonly observed trade-off phenomena between nonlinearity and stability observed in typical thermal, crosslinkable materials – which hamper the full potential of high optical nonlinearity in these materials – we suggested a new modified poling/photocuring process.

4. Conclusions

The introduction of a photocrosslinkable moiety constitutes a new approach to obtain highly efficient NLO star-shaped molecules. The relatively high EO coefficients under a low poling field and the tunability of thermal stability offer the advantage of overcoming the trade-off between nonlinearity and stability, notably, the degradation of the chromophore during UV irradiation in the presence of radical species. The TCP-based chromophore used in this study shows significant opposition to radicals that are generated in the material. When **6a** was poled under a field of 80 V/μm, the maximum EO coefficient was ~37.0 pm/V; **6b** exhibited much improved stability after UV irradiation.

Acknowledgments

This work was supported by the Korea Research Foundation (Fundamental Research Program, R0606661, 2006). Particularly, Prof. Dong Hoon Choi thanks the Seoul R&BD Program (2006–2007).

References

[1] Casalboni M, Caruso U, De Maria A, Fusco M, Panunzi B, Quatela A, et al. J Polym Sci Part A Polym Chem 2004;42:3013.
[2] Hua JL, Li Z, Long K, Qin JG, Li SJ, Ye C, et al. J Polym Sci Part A Polym Chem 2005;43:1317.
[3] Briers D, Koeckelberghs G, Picard I, Verbiest T, Persoons A, Samyn C. Macromol Rapid Commun 2003;24:841.
[4] Balakrishnan M, Faccini M, Diemeer MBJ, Verboom W, Driessen A, Reinhoudt DN, et al. Electron Lett 2006;42:51.
[5] Kim SK, Hung YC, Seo BJ, Geary K, Yuan W, Bortnik B, et al. Appl Phys Lett 2005;288:061112-1.
[6] Park S, Ju JJ, Park SK, Lee MH, Do JY. Appl Phys Lett 2005;86:071102.
[7] Shi Y, Zhang C, Zhang H, Betchel JH, Steier WH, Robinson B, et al. Science 2000;288:119.
[8] Lacroix PG. Chem Mater 2001;13:3495.
[9] Katti KV, Raghuraman K, Pillarsetty N, Karra SR, Gulotty RJ, Chartier MA, et al. Chem Mater 2002;14:2436.

[10] Zhu P, van der Boom ME, Kang H, Evmenenko G, Dutta P, Marks TJ. Chem Mater 2002;14:4982.
[11] Luo J, Cheng YJ, Kim TD, Hau S, Jang SH, Shi Z, et al. Org Lett 2006;8:1387.
[12] Marks TJ, Ratner MA. Angew Chem Int Ed Eng 1995;34:155.
[13] Kajzar F, Lee KS, Jen AKY. Adv Polym Sci 2003;161:1.
[14] Zhang C, Wang C, Yang J, Dalton LR, Sun G, Zhang H, et al. Macromolecules 2001;34:235.
[15] Ma H, Wu J, Herguth P, Chen B, Jen AKY. Chem Mater 2000;12:1187.
[16] Jang SH, Luo J, Tucker NM, Leclercq A, Zojer E, Haller MA, et al. Chem Mater 2006;18:2982.
[17] Yin S, Xu H, Su X, Li G, Song Y, Lam J, et al. Polym Sci Part A Polym Chem 2006;44:2346.
[18] Smitha P, Asha SK, Pillai CKS. J Polym Sci Part A Polym Chem 2005;43:4455.
[19] Cho MJ, Kim GW, Jun WG, Lee SK, Jin JI, Choi DH. Thin Solid Films 2006;500:52.
[20] Sullivan PA, Akelaitis AJP, McGrew G, Lee SK, Choi DH, Dalton LR. Chem Mater 2006;18:344.
[21] Michelotti F, Toussaere E, Levenson R, Liang J, Zyss J. J Appl Phys 1996;80:1773.
[22] Teng CC, Man HT. Appl Phys Lett 1990;56:1734.
[23] Choi DH, Oh SJ, Cha HB, Lee JY. Eur Polym J 2001;37:1951.
[24] Choi DH, Cha YK. Polymer 2002;43:703.
[25] Lee BH, Kim JH, Cho MJ, Lee SH, Choi DH. Dyes Pigments 2004;61:235.